(International Print/Online Journal)

SJIF IMPACT FACTOR: 6.829
PUBMED-National Library of Medicine ID-101739732

ISSN (Print): 2209-2870
ISSN (Online): 2209-2862

International Journal of Medical Science and Current Research (IJMSCR)
Available online at: www.ijmscr.com
Volume 8, Issue 6 , Page No: 445-459
November-December 2025

IJMSCR

Neuroimaging Patterns in Toxic and Metabolic Encephalopathies: A Case Series Study

[1]Dr. Lavisha Khandelwal, [2]Dr. Adarsh B H, [3]Dr. Avinash M Katur
[1]PG Resident, [2,3]Assistant Professor
Department of Radiodiagnosis, JJM Medical College, Davangere

***Corresponding Author:**
Dr. Lavisha Khandelwal
PG Resident, Department of Radiodiagnosis, JJM Medical College, Davangere

Type of Publication: Original Research Paper
Conflicts of Interest: Nil

Abstract

Background:
Toxic and metabolic encephalopathies represent a diverse group of reversible neurological disorders arising from systemic metabolic derangements, organ dysfunction, or exposure to neurotoxins.
Clinical presentation is often nonspecific, making neuroimaging-particularly MRI-crucial for early detection and differentiation.

Methods:
This retrospective study conducted at JJM Medical College (January-April 2025) included 12 patients diagnosed with toxic or metabolic encephalopathy. Patients with trauma,
infection, neoplasm, or incomplete imaging were excluded. MRI was performed using a 1.5T Philips Achieva scanner with standard sequences (T1, T2, FLAIR, DWI, ADC, SWI) and contrast when indicated; MR spectroscopy was performed in selected cases. Imaging findings were analyzed for lesion distribution, symmetry, and diffusion characteristics and correlated with clinical and laboratory data.

Results:
Twelve representative cases demonstrated distinct MRI patterns: hepatic encephalopathy (globus pallidus T1 hyperintensity), uremic encephalopathy ("lentiform fork sign"), snakebite toxicity (bilateral basal ganglia changes), Wernicke's encephalopathy (medial thalamic lesions), hyperammonemic encephalopathy (cingulate and insular diffusion restriction), hypoglycemic encephalopathy (occipital involvement), posterior reversible encephalopathy syndrome (parieto- occipital vasogenic edema), hypoxic-ischemic encephalopathy (neonatal periventricular restriction), cytotoxic lesions of the corpus callosum (CLOCCs), osmotic demyelination syndrome (pontine "trident sign"), uremic leukoencephalopathy (periventricular restriction), and hypoparathyroid encephalopathy (basal ganglia and white matter calcifications).

Conclusion:
A pattern-based MRI approach, integrated with clinical and biochemical data, enables early recognition of toxic and metabolic encephalopathies, guiding prompt treatment and improving neurological outcomes.

Keywords: Metabolic encephalopathy, Toxic encephalopathy, Hepatic encephalopathy, Neuroimaging, Wernicke's encephalopathy,

Introduction

Toxic and metabolic encephalopathies comprise a diverse group of brain disorders resulting from systemic metabolic disturbances, including organ failure, toxin exposure, electrolyte abnormalities, and nutritional deficiencies [1,2]. Their clinical presentation ranges from mild confusion to seizures, coma, and potentially permanent neurological deficits. Because these manifestations are often nonspecific,

establishing an early etiological diagnosis in acute care settings can be challenging

[1-3]. Magnetic resonance imaging (MRI) plays a pivotal role in evaluation, as it can identify characteristic injury patterns across the cortex, deep gray nuclei, white matter, and posterior fossa. Moreover, MRI assessment of diffusion and vascular abnormalities helps narrow the differential diagnosis, directly influencing the urgency of laboratory investigations and guiding timely treatment decisions [4-6].

Several reproducible MRI phenotypes are associated with toxic-metabolic insults. Chronic hepatic encephalopathy typically demonstrates T1 hyperintensity of the bilateral globus pallidus due to manganese deposition, often accompanied by white matter signal alterations [7]. Uremic encephalopathy frequently involves the basal ganglia and periventricular white matter, sometimes presenting with the classic "lentiform fork sign" [7-9]. Thiamine deficiency, as seen in Wernicke's encephalopathy, preferentially affects the medial thalami, mammillary bodies, and periaqueductal gray on FLAIR/T2 and DWI sequences; when suspected, rapid empiric treatment is imperative [10,11]. Hyperammonemic encephalopathy commonly targets the cingulate and insular cortices with diffusion restriction, whereas hypoglycemia tends to injure the parieto-occipital cortex, producing gyriform diffusion abnormalities—patterns that help differentiate metabolic injury from hypoxic-ischemic encephalopathy [12-15].

Other important conditions include posterior reversible encephalopathy syndrome (PRES), characterized by posterior subcortical vasogenic edema; osmotic demyelination syndrome (ODS), marked by central pontine "trident/omega" changes following rapid sodium correction; cytotoxic lesions of the corpus callosum (CLOCCs); and a range of toxic leukoencephalopathies associated with medications, environmental toxins, and uremia [16-18]. In India, region-specific health burdens—such as snake envenomation, malnutrition, alcohol-related thiamine deficiency, and untreated renal or hepatic disease—further broaden the spectrum of imaging findings and heighten the relevance of MRI pattern recognition for rapid triage and targeted management [19-23].

This retrospective case series from JJM Medical College examines 12 patients with toxic and metabolic encephalopathies, correlating their MRI patterns with clinical and laboratory parameters . The study highlights a pattern-based MRI approach that expedites diagnosis and enhances the potential for neurological recovery by emphasizing consistent imaging signatures across hepatic, uremic, hyperammonemic, hypoglycemic, and Wernicke's encephalopathies, as well as PRES, osmotic demyelination, CLOCCs, neonatal HIE, toxic leukoencephalopathy, and hypoparathyroid encephalopathy [22-30].

Materials And Methods:

This retrospective study conducted at JJM Medical College (January-April 2025) included 12 patients diagnosed with toxic or metabolic encephalopathy. Patients with trauma, infection, neoplasm, or incomplete imaging were excluded. MRI was performed using a 1.5T Philips Achieva scanner with standard sequences [T1, T2, Fluid-Attenuated Inversion Recovery (FLAIR), Diffusion-Weighted Imaging (DWI), Apparent Diffusion Coefficient (ADC), Gradient Recalled Echo (GRE)] and contrast when indicated; MR spectroscopy was performed in selected cases.

Imaging findings were analyzed for lesion distribution, symmetry, and diffusion characteristics and correlated with clinical and laboratory data.

Results:

Case 1:

A 40-year-old male with a long-standing history of chronic alcohol use presented with altered sensorium and involuntary movements. An initial non-contrast CT scan showed no acute abnormalities. Subsequent MRI demonstrated symmetrical T1 hyperintensities in the bilateral globus pallidus (Fig. 1A & 1B) along with T2/FLAIR hyperintensity involving the corticospinal tracts (Fig. 1C & 1D). These imaging findings were characteristic of **chronic hepatic encephalopathy** [1,2]. Abdominal ultrasonography (Fig. 2) further supported the diagnosis, revealing features of cirrhosis and portal hypertension.

Volume 8, Issue 6; November-December 2025; Page No 445-459

Figure 1: MRI Findings in Hepatic Encephalopathy. Fig. 1A & 1B: Axial and coronal T1-weighted images showing symmetrical hyperintensities in the bilateral globus pallidus. Fig. 1C & 1D: Axial FLAIR images demonstrating hyperintensity along the corticospinal tracts

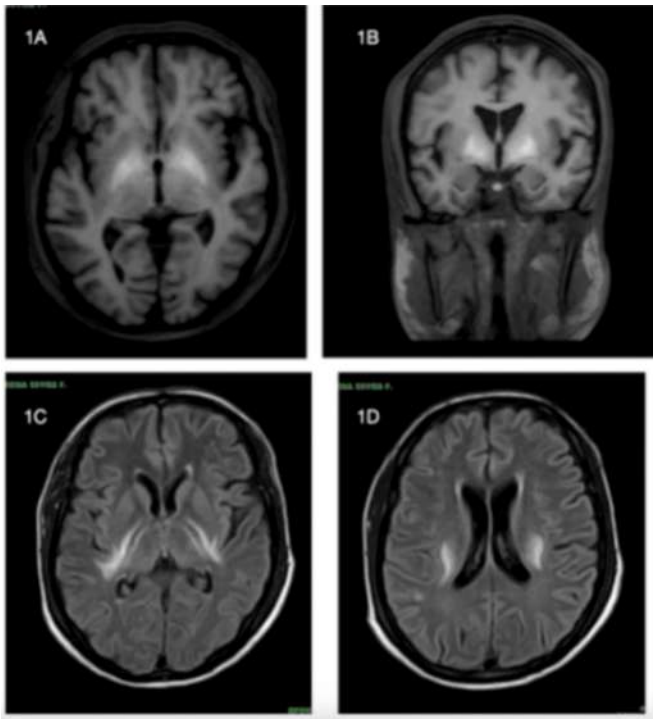

Figure 2: Ultrasound images show coarsened hepatic echotexture, irregular surface margins, and peri-hepatic ascites—findings suggestive of chronic liver parenchymal disease.

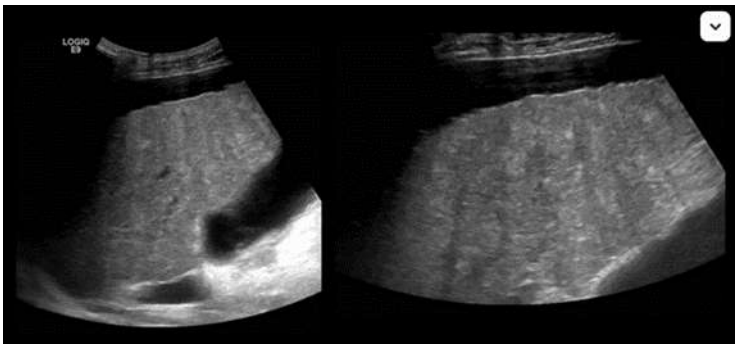

Case 2:

A 30-year-old male presented with seizures and altered sensorium. MRI of the brain showed T2- weighted and FLAIR hyperintensity in the periventricular white matter extending into the external and internal capsules around the lentiform nucleus (Fig. 3). This configuration formed the classic **"lentiform fork sign,"** characteristic of **uremic toxic encephalopathy** [1]. Renal function tests revealed elevated urea and creatinine levels, confirming metabolic encephalopathy secondary to uremia.

Volume 8, Issue 6; November-December 2025; Page No 445-459

Figure 3: Axial T2-weighted and FLAIR images demonstrate hyperintensity in the periventricular white matter, extending into the external and internal capsules surrounding the lentiform nucleus, producing the characteristic "lentiform fork sign" typical of uremic encephalopathy.

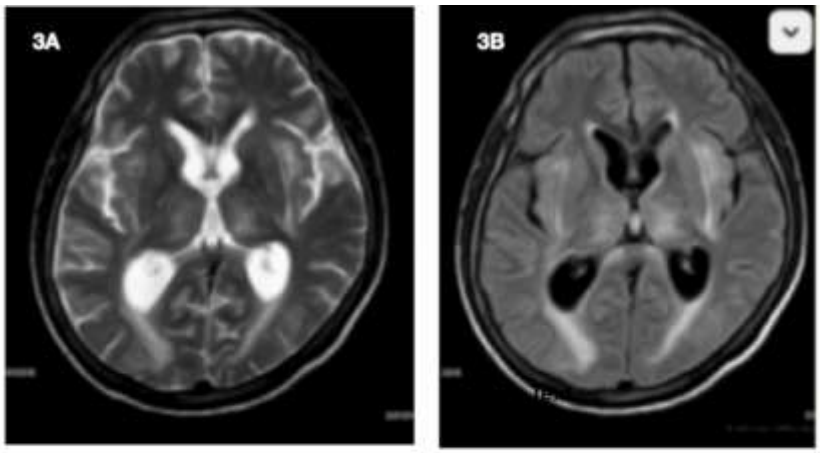

Investigation	Result	Unit	Normal
Urea (Serum)	73.9	mg/dL	7-20 mg/dL
Creatinine (Serum)	2.2	mg/dL	0.6-1.3 mg/dL

A similar presentation was observed in a 50-year-old male who also reported altered sensorium. Laboratory investigations revealed elevated serum creatinine (6.2 mg/dL) and urea (116 mg/dL). MRI of the brain showed symmetrical T2/FLAIR hyperintensity with corresponding T1 hypointensity involving the bilateral caudate and lentiform nuclei (Fig. 4), again forming the "lentiform fork sign" and confirming uremic encephalopathy.

Figure 4: MRI images demonstrate symmetrical T2/FLAIR hyperintensity with corresponding T1 hypointensity in the bilateral caudate and lentiform nuclei, producing the characteristic "lentiform fork sign," indicative of uremic encephalopathy.

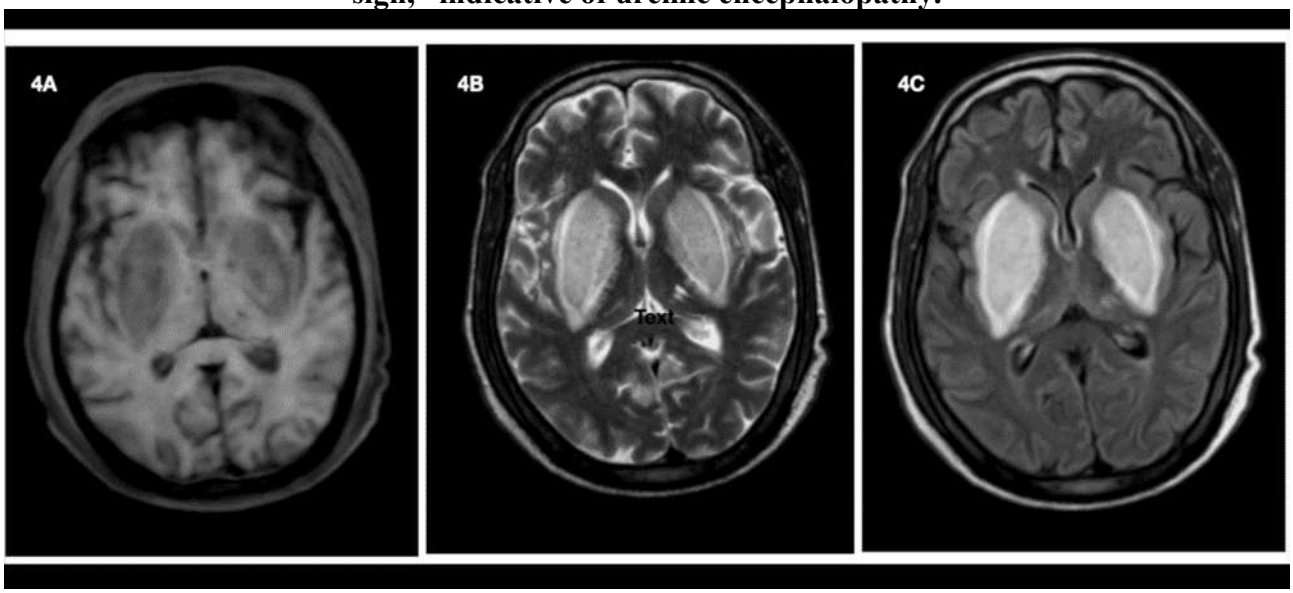

Volume 8, Issue 6; November-December 2025; Page No 445-459

Case 3:

A 6-year-old male presented with altered sensorium two days after a cobra bite. MRI of the brain demonstrated symmetrical T2-weighted and FLAIR hyperintensities involving the bilateral caudate nuclei and putamina (Fig. 5). There was no diffusion restriction on DWI and no susceptibility blooming on GRE sequences. This pattern is characteristic of **snakebite-induced toxic encephalopathy** [3].

Figure 5: Axial FLAIR and T2-weighted images showing bilateral symmetrical hyperintensities in the caudate nuclei and putamina.

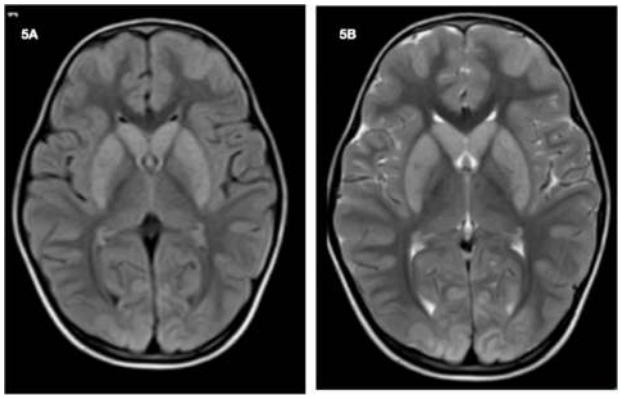

Case 4:

A 45-year-old patient with a history of chronic alcoholism presented with confusion and ataxia. MRI of the brain revealed symmetrical T2-weighted and FLAIR hyperintensities involving the bilateral medial thalami and regions adjacent to the third ventricle (Fig. 6). Laboratory evaluation showed reduced serum thiamine levels.

These imaging findings are characteristic of **Wernicke's encephalopathy**, which classically involves the medial thalami, mammillary bodies, hypothalamus, tectal plate, peri-aqueductal gray matter, and putamina [1].

Figure 6: Axial T2-weighted and FLAIR images demonstrate symmetrical hyperintensities in the bilateral medial thalami and regions adjacent to the third ventricle, consistent with Wernicke's encephalopathy.

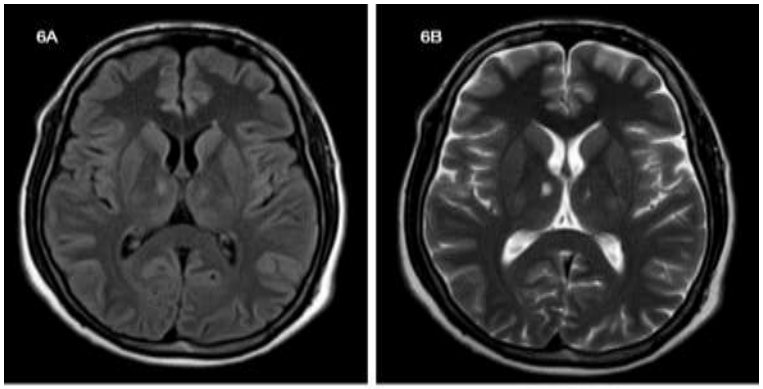

Case 5:

A 56-year-old male presented with altered mental status and disorientation. Laboratory evaluation revealed elevated serum ammonia levels. MRI of the brain showed bilateral and symmetrical diffusion restriction predominantly involving the insular and cingulate gyri, with sparing of the occipital lobes (Fig. 7A & 7B). Subtle

Volume 8, Issue 6; November-December 2025; Page No 445-459

FLAIR hyperintensities were observed in the same regions (Fig. 7C), and GRE sequences showed no susceptibility blooming (Fig. 7D).

These imaging features are characteristic of **hyperammonemic encephalopathy**. MR spectroscopy, when performed, may demonstrate an elevated glutamate–glutamine peak between 2.1 and 2.4 ppm, further supporting the metabolic etiology [1].

Figure 7: Fig. 7A & 7B: Axial DWI and ADC images showing bilateral, symmetrical diffusion restriction involving the insular and cingulate gyri with occipital sparing. Fig. 7C: Corresponding FLAIR image demonstrating hyperintensity in the same regions. Fig. 7D: GRE sequence showing no susceptibility blooming. These findings are consistent with hyperammonemic encephalopathy.

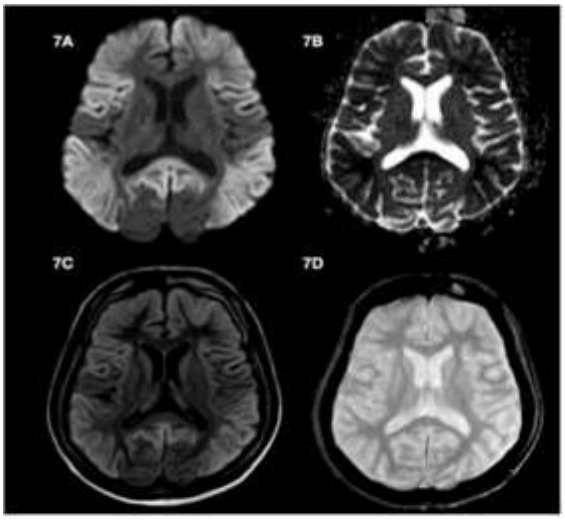

PARAMETER	RESULT	REFERENCE
Serum ammonia	87 micromol/L	15-45 micromol/L

Case 6:

A 38-year-old insulin-dependent male presented to the emergency department with altered mental status and loss of consciousness. On arrival, his blood glucose level was critically low at 28 mg/dL. Axial FLAIR MRI images showed symmetrical hyperintensities in the bilateral occipital lobes (Fig. 8), with corresponding diffusion restriction on DWI and ADC sequences.

These imaging features are characteristic of **hypoglycemic encephalopathy**, which typically presents with symmetrical T2/FLAIR hyperintensities and marked diffusion restriction, predominantly affecting the cortical gyri of the parieto-occipital and temporal lobes. Basal ganglia involvement may be seen but is associated with poorer prognosis, while the thalami, white matter, and cerebellum are usually spared [2].

Volume 8, Issue 6; November-December 2025; Page No 445-459

Figure 8: Axial FLAIR MRI shows symmetrical hyperintensities in the bilateral occipital lobes. Corresponding DWI and ADC images demonstrate diffusion restriction in the same regions, consistent with hypoglycemic encephalopathy.

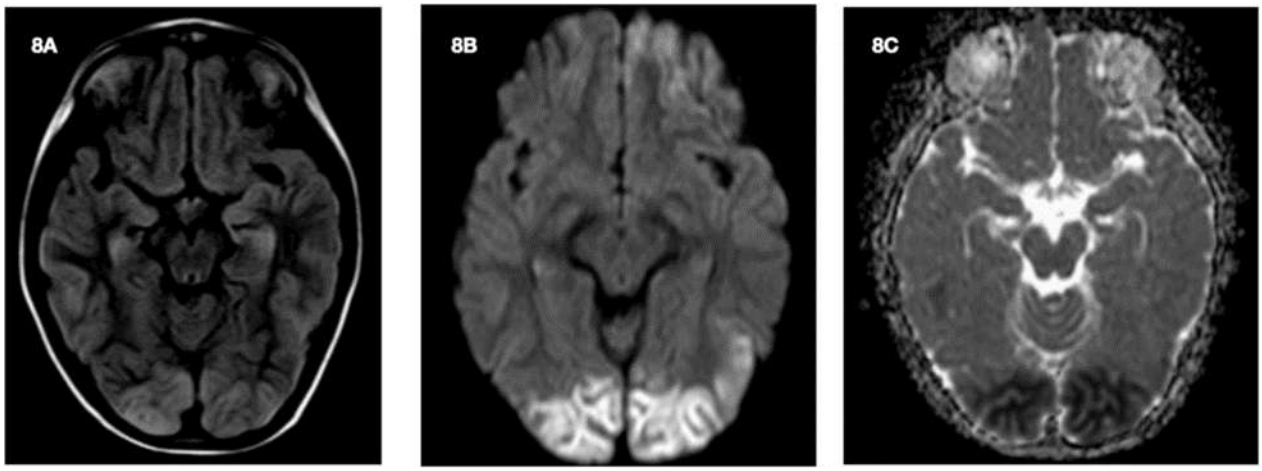

Case 7:

A 29-year-old primigravida at 32 weeks of gestation presented with sudden-onset seizures and visual disturbances. Her blood pressure on admission was 190/100 mmHg. MRI of the brain revealed T2-weighted and FLAIR hyperintensities in the bilateral occipital and posterior parietal lobes (Fig. 9). Diffusion-weighted imaging showed no significant diffusion restriction, consistent with vasogenic edema, and GRE sequences demonstrated no evidence of hemorrhage. These imaging features are characteristic of **posterior reversible encephalopathy syndrome (PRES)**[1].

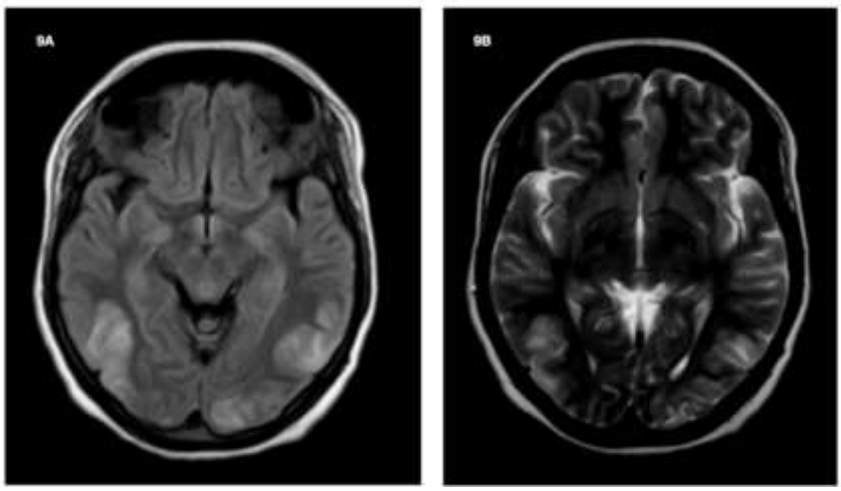

Figure 9: Axial T2-weighted and FLAIR images show symmetrical hyperintensities in the bilateral occipital and posterior parietal lobes, consistent with posterior reversible encephalopathy syndrome (PRES).

Volume 8, Issue 6; November-December 2025; Page No 445-459

Case 8:

A full-term male neonate was delivered via emergency cesarean section due to prolonged labor and fetal bradycardia. Within the first 12 hours of life, the infant developed hypotonia and seizures.

Laboratory studies revealed metabolic acidosis and elevated lactate levels. MRI performed on day 4 of life showed diffusion restriction in the bilateral periventricular and supraventricular regions (Fig. 10), with corresponding subtle hyperintensity on FLAIR sequences. These imaging findings are consistent with **hypoxic-ischemic encephalopathy.**

Figure 10: Axial DWI and ADC images demonstrate diffusion restriction in the bilateral periventricular and supraventricular regions. Corresponding FLAIR images show subtle hyperintensity in the same areas, consistent with hypoxic-ischemic encephalopathy.

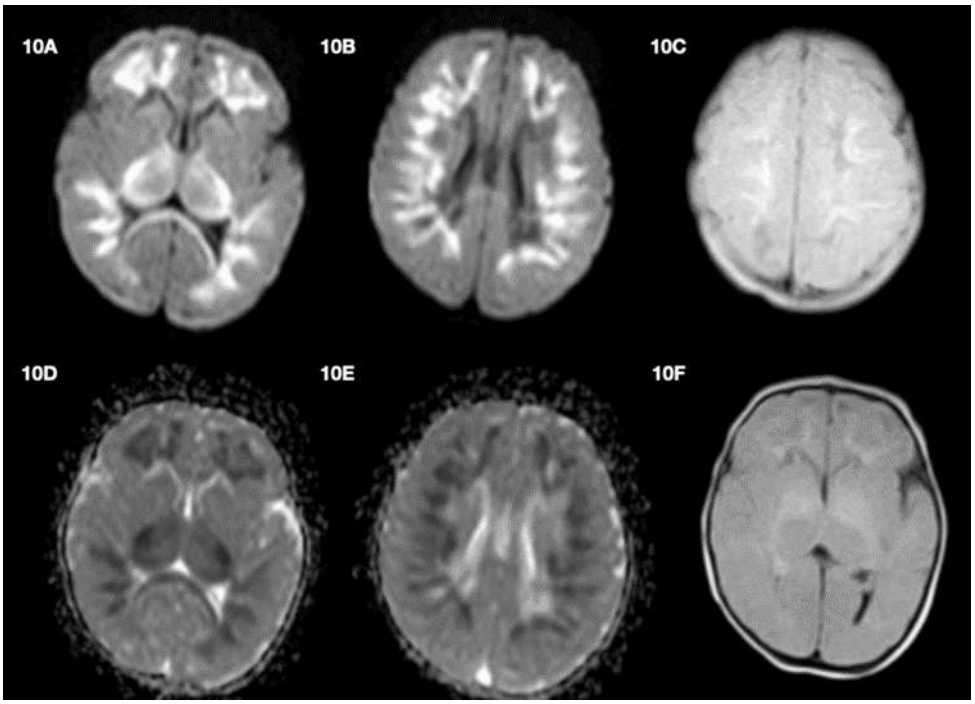

Volume 8, Issue 6; November-December 2025; Page No 445-459

Case 9:

An 11-month-old infant presented to the emergency department with generalized seizures and lethargy. MRI of the brain demonstrated restricted diffusion involving the splenium and genu of the corpus callosum (Fig. 11). There was no evidence of hemorrhage or post-contrast enhancement.

These imaging findings are characteristic of **cytotoxic lesions of the corpus callosum (CLOCCs)**, a transient phenomenon often associated with metabolic or infectious encephalopathy.

Figure 11: Axial DWI images demonstrate restricted diffusion in the splenium and genu of the corpus callosum, consistent with cytotoxic lesions of the corpus callosum (CLOCCs).e

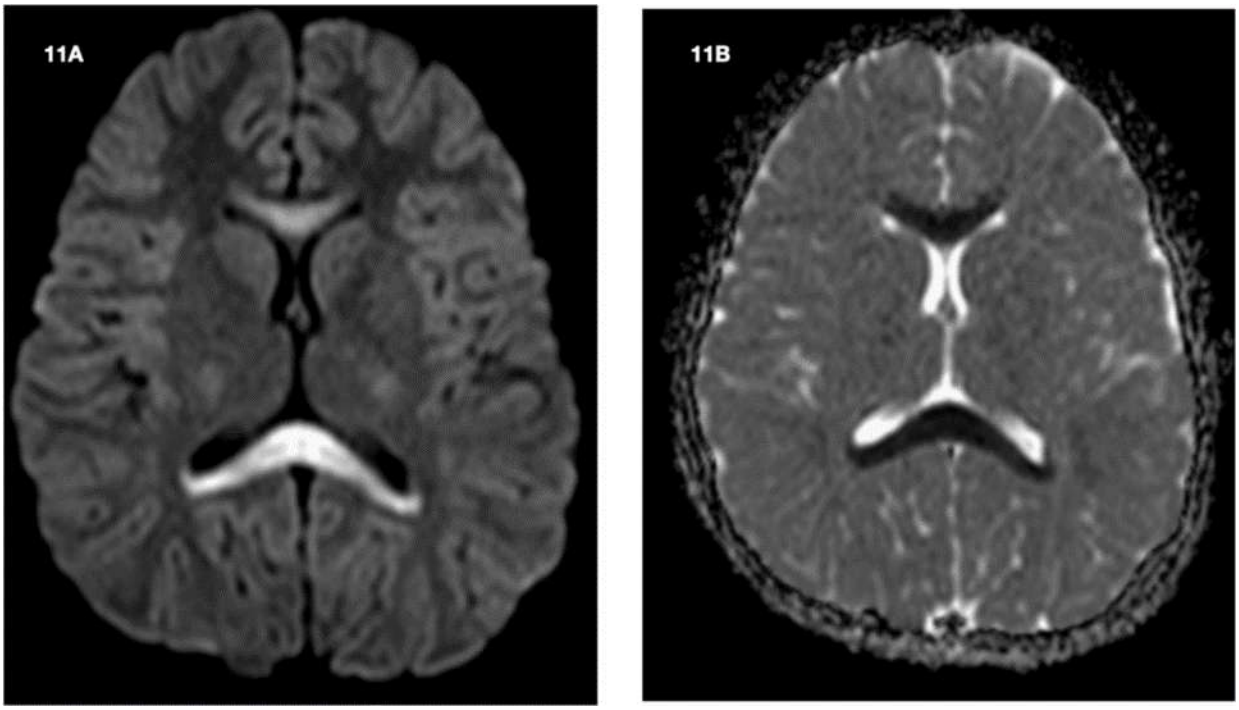

Case 10:

A 50-year-old female presented with altered sensorium. On admission, her serum sodium level was 110 mmol/L. Following rapid correction of hyponatremia to 135 mmol/L, she developed dysarthria and fluctuating consciousness.

MRI of the brain revealed T2-weighted and FLAIR hyperintensity in the central pons with relative sparing of peripheral pontine fibers, producing the characteristic "trident-shaped" appearance (Fig. 12). There was no diffusion restriction, susceptibility blooming on GRE sequences, or contrast enhancement [2].

These findings are consistent with **osmotic demyelination syndrome**, commonly occurring after rapid correction of hyponatremia, reflecting the susceptibility of pontine oligodendrocytes to abrupt osmotic shifts.

Volume 8, Issue 6; November-December 2025; Page No 445-459

Figure 12: Axial T2-weighted and FLAIR images demonstrate central pontine hyperintensity with sparing of peripheral fibers, producing the characteristic "trident sign," consistent with osmotic demyelination syndrome.

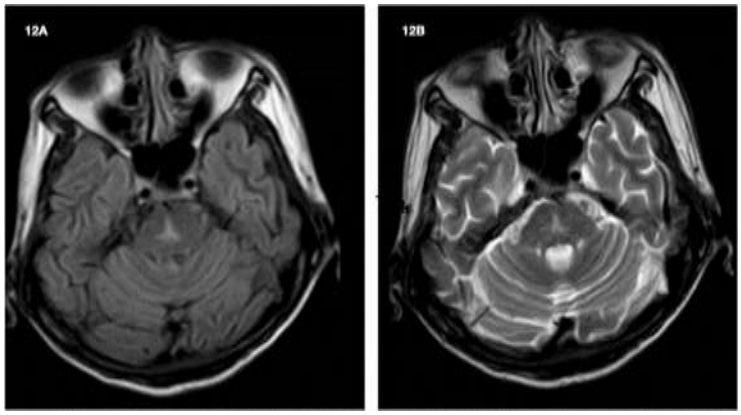

Case 11:

A 46-year-old male with chronic kidney disease, who had missed multiple dialysis sessions, presented with progressive confusion, slurred speech, and decreased responsiveness over 48 hours. Laboratory investigations revealed markedly elevated serum urea and creatinine levels.

MRI of the brain showed diffuse, bilateral, and symmetrical diffusion restriction in the periventricular and supraventricular white matter (Fig. 13), with corresponding subtle FLAIR hyperintensity.

These findings are consistent with **acute toxic leukoencephalopathy**, likely secondary to uremic toxin accumulation due to renal failure. Other common causes of acute leukoencephalopathy include chemotherapeutic agents (e.g., methotrexate), opioid toxicity (e.g., heroin), carbon monoxide poisoning, and immunosuppressive medications (e.g., cyclosporine, tacrolimus). These conditions typically produce bilateral, symmetrical white matter changes on MRI, often with diffusion restriction, and may be reversible with prompt recognition and management.

Figure 13: Axial DWI and ADC images demonstrate bilateral, symmetrical diffusion restriction in the periventricular and supraventricular white matter. Corresponding FLAIR images show subtle hyperintensity in the same regions, consistent with acute toxic/uremic leukoencephalopathy.

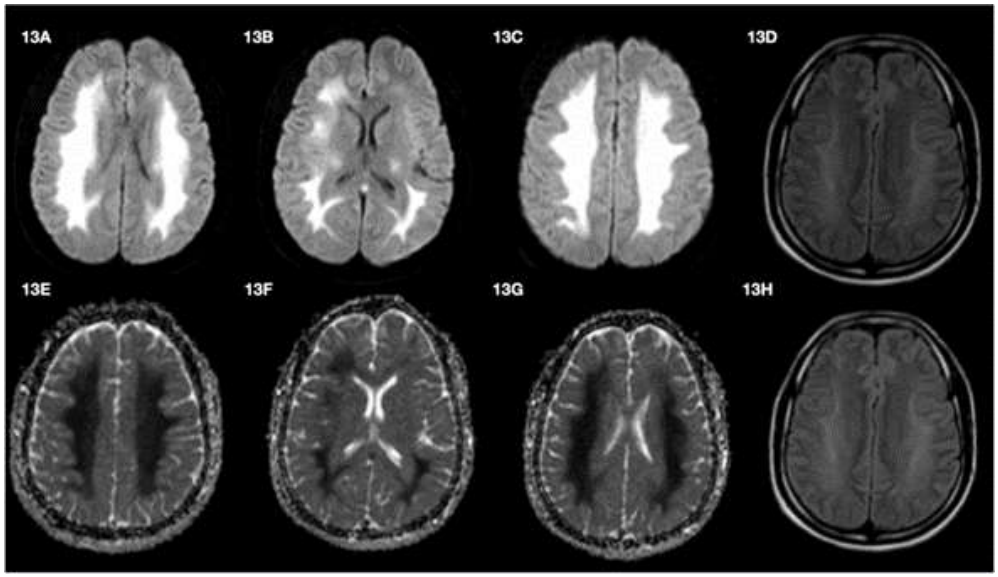

Volume 8, Issue 6; November-December 2025; Page No 445-459

Case 12: A 45-year-old female presented with altered sensorium. Non-contrast CT of the brain demonstrated bilateral, symmetrical hyperdensities (HU: 70) in the caudate nuclei, globus pallidus, and putamen (lentiform nuclei) (Fig. 14). MRI revealed corresponding bilateral, symmetrical T1 hyperintensities in the basal ganglia, with susceptibility blooming on GRE sequences. No diffusion restriction was observed on DWI. These imaging findings are consistent with **hypoparathyroid encephalopathy.**

Figure 14: Non-contrast CT brain shows bilateral, symmetrical hyperdensities in the caudate nuclei, globus pallidus, and putamen (lentiform nuclei). Axial T1-weighted MRI images demonstrate corresponding bilateral, symmetrical hyperintensities in the basal ganglia with susceptibility blooming on GRE sequences, consistent with hypoparathyroid encephalopathy.

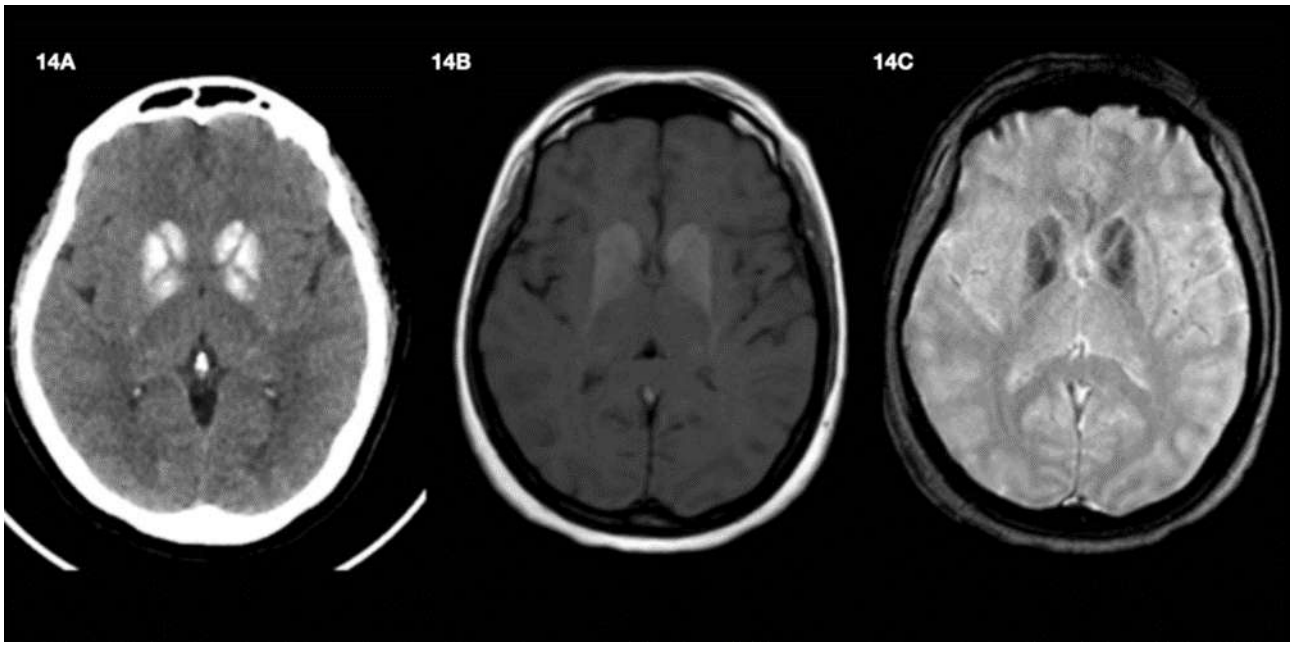

Discussion:

Toxic and metabolic encephalopathies constitute a broad spectrum of neurologic disorders characterized by global cerebral dysfunction, commonly presenting as altered mental status, confusion, or acute delirium. These conditions are frequently encountered in emergency and critical care settings and often pose significant diagnostic challenges due to nonspecific clinical presentations. Early recognition is crucial, as many of these disorders are potentially reversible with timely, targeted intervention.

The central nervous system (CNS) is particularly vulnerable to metabolic disturbances and circulating toxins due to its high metabolic demands and limited energy reserves. Even brief biochemical imbalances or toxin exposure can result in widespread cerebral dysfunction. While clinical features alone may be insufficient for etiology-specific diagnosis, neuroimaging— especially MRI—plays a central role in narrowing the differential diagnosis, guiding further evaluation, and providing prognostic information. Characteristic imaging features include bilateral and symmetric lesions, diffusion restriction, minimal or absent mass effect, and lack of contrast enhancement. Diffusion-weighted imaging (DWI) is especially sensitive for detecting early cytotoxic injury.

The distribution and pattern of abnormalities often reflect underlying pathophysiology. When interpreted alongside clinical and laboratory data, these patterns can help identify specific causes. Key neuroimaging patterns include:

Basal Ganglia and/or Thalamic Involvement

The basal ganglia and thalami are highly metabolically active, making them susceptible to cytotoxic injury. Involvement often indicates severe metabolic

Volume 8, Issue 6; November-December 2025; Page No 445-459

disturbance and is associated with poor prognosis. Three sub-patterns are recognized:

1. Pattern A – T2/FLAIR hyperintensity: Wernicke's encephalopathy, methanol and carbon monoxide poisoning, uremic encephalopathy, vigabatrin toxicity.
2. Pattern B – T2 hypointensity: Chronic toluene toxicity, hypoparathyroidism, and other parathyroid disorders.
3. Pattern C – T1 hyperintensity: Chronic hepatic encephalopathy, total parenteral nutrition-associated encephalopathy, diabetic striatopathy (typically unilateral).

Dentate Nuclei Involvement

Bilateral lesions in the cerebellar dentate nuclei suggest specific toxic exposures, most notably metronidazole toxicityand methyl bromide poisoning. These lesions are potentially reversible with early cessation of the offending agent.

Prominent Cortical Gray Matter Involvement

Extensive cortical involvement with diffusion restriction is seen in hypoglycemic encephalopathy, hypoxic-ischemic injury, and hyperammonemic encephalopathy. This pattern typically indicates advanced injury and is associated with higher morbidity.

Symmetric Periventricular White Matter Involvement with Gray Matter Sparing

Classic for acute toxic leukoencephalopathy (ATL), this pattern reflects intramyelinic edema rather than true demyelination. Etiologies include chemotherapy agents (methotrexate, 5-FU), immunosuppressants, and illicit drug use (e.g., heroin inhalation). Prognosis is generally favorable and reversible upon removal of the offending agent.

Corticospinal Tract Involvement

Lesions along the corticospinal tracts, including internal capsules and brainstem, suggest mitochondrial disorders (e.g., Leigh syndrome), inherited leukodystrophies, or vitamin B12 deficiency. In B12 deficiency, cervical spine MRI shows the characteristic "inverted V" sign on T2- weighted imaging due to dorsal and lateral column involvement (Fig. 15).

Figure 15: Axial T2- weighted MRI images of the cervical spinal cord demonstrating the characteristic "inverted V" sign (arrow) in the dorsal and lateral columns. This pattern is indicative of subacute combined degenerations of the spinal cord commonly seen in vitamin B12 (cobalamin) deficiency.

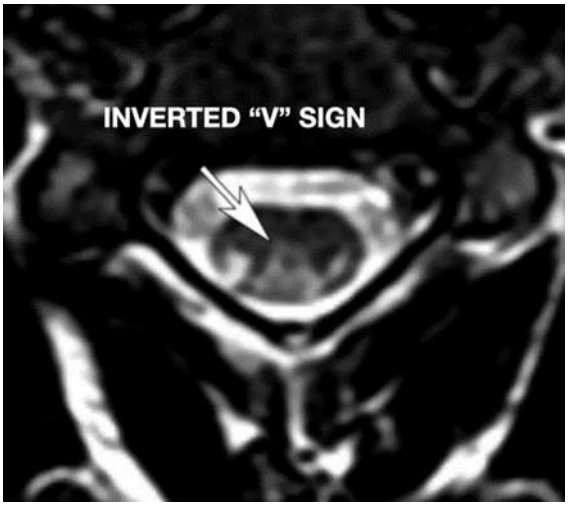

Volume 8, Issue 6; November-December 2025; Page No 445-459

Figure 16: Sagittal T1 weighted MRI images of the corpus callosum showing selective involvement of the middle layers, producing the characteristic "sandwich sign" (arrow).

This pattern is typically seen in Marchiafava- Bignami disease.

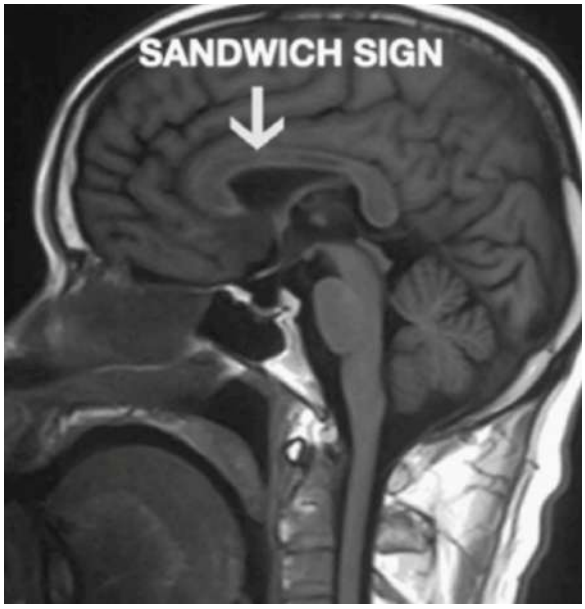

Figure 17: Axial T2 weighted and FLAIR MRI images of the pons demonstrating the classic "trident sign", characterised by central pontine hyperintensity with relative sparing of the peripheral pontine fibres. This finding is diagnostic of central pontine myelinolysis, typically secondary to rapid correction of severe hyponatremia.

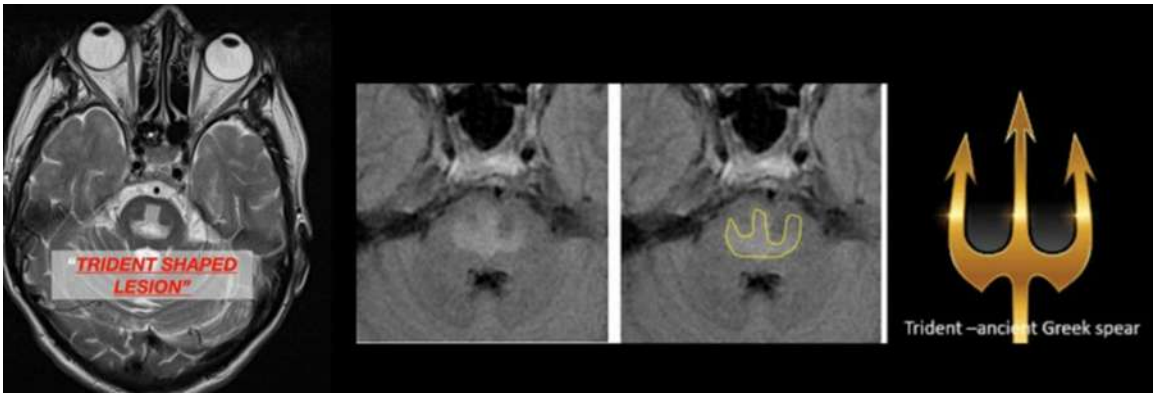

Corpus Callosum Involvement

Splenial lesions are observed in Marchiafava-Bignami disease, alcohol-related encephalopathy, and antiepileptic drug toxicity. In Marchiafava-Bignami disease, selective involvement of the middle corpus callosum layers produces the "sandwich sign" on imaging (Fig. 16). Reversibility depends on etiology and clinical status.

Asymmetric White Matter Lesions In A Demyelinating Pattern

While classic in primary demyelinating disorders, asymmetric white matter lesions can occur in metabolic leukodystrophies such as adrenoleukodystrophy and Krabbe disease. Differentiation requires careful evaluation of onset, progression, and metabolic profiles.

Parieto-Occipital Subcortical Vasogenic Edema

Characteristic of posterior reversible encephalopathy syndrome (PRES), triggered by severe hypertension, renal failure, eclampsia, or cytotoxic medications.

Volume 8, Issue 6; November-December 2025; Page No 445-459

MRI shows vasogenic edema in parieto-occipital subcortical white matter, which is usually reversible with timely intervention.

Central Pontine Involvement

Central pontine myelinolysis (CPM), a form of osmotic demyelination, arises from rapid correction of severe hyponatremia. Risk factors include serum sodium <115 mmol/L or correction >12 mmol/ L/day. MRI shows a symmetrical, well-demarcated, trident-shaped lesion in the central pons, sparing peripheral fibers and corticospinal tracts (Fig. 17).

Radiologic features are often nonspecific and can overlap across etiologies. Integration of MRI patterns with clinical history, laboratory data (metabolic panels, liver/kidney function, serum ammonia, toxicology screens), and electrophysiologic studies is essential. This multidisciplinary, pattern-based approach enhances diagnostic accuracy, guides timely initiation of etiology-specific treatment, and informs prognosis. Certain imaging patterns, such as white matter sparing with intramyelinic edema, are more likely reversible, whereas deep gray matter cytotoxic injuryusually indicates poorer outcomes.

Conclusion:

Toxic and metabolic encephalopathies remain diagnostically challenging due to their nonspecific clinical presentations and considerable overlap in neuroimaging appearances. However, recognition of characteristic MRI patterns—particularly when correlated with clinical context, metabolic profiles, and relevant exposure history—provides a powerful and efficient diagnostic framework.

Early identification of these imaging signatures allows clinicians to initiate timely, etiology-specific treatment, which is critical for preventing irreversible neurological injury. Importantly, several of these conditions demonstrate substantial potential for reversibility when promptly addressed. A systematic, pattern-based approach that integrates imaging with multidisciplinary clinical assessment therefore plays a key role in improving patient outcomes in both emergency and critical care settings.

References:

1. Le Guennec L, Marois C, Demeret S, Wijdicks EFM, Weiss N: Toxic-metabolic encephalopathy in adults: Critical discussion and pragmatical diagnostic approach. Rev Neurol (Paris. 2022, 178:93-104. 10.1016/j.neurol.2021.11.007
2. Sharma P, Eesa M, Scott JN: Toxic and acquired metabolic encephalopathies: MRI appearance. AJR Am J Roentgenol. 2009, 193:879-886. 10.2214/AJR.08.2257
3. Kim Y, Kim JW: Toxic encephalopathy. Saf Health Work. 2012, 3:243-56. 10.5491/ SHAW.2012.3.4.243
4. Ozütemiz C, Roshan SK, Kroll NJ, et al.: Acute Toxic Leukoencephalopathy: Etiologies, Imaging Findings, and Outcomes in 101 Patients. AJNR Am J Neuroradiol. 2019, 40:267-275. 10.3174/ajnr.A5947
5. Rovira A, Alonso J, Córdoba J: MR imaging findings in hepatic encephalopathy. AJNR Am J Neuroradiol. 2008, 29:1612-21. 10.3174/ajnr.A1139
6. Lim CG, Hahm MH, Lee HJ: Hepatic encephalopathy on magnetic resonance imaging and its uncertain differential diagnoses: a narrative review. J Yeungnam Med Sci. 2023, 40:136-145. 10.12701/jyms.2022.00689
7. Narra RK: Lentiform fork sign in uraemic encephalopathy. BMJ Case Rep. 2021, 17:245623. 10.1136/bcr-2021-245623
8. Alhusseini A, Hamsho S, Alabdullah H, Alaswad M, Sleiay M, Alsamarrai O: Uremic encephalopathy manifesting with a unique MRI finding (the lentiform fork sign) in an adult male: A case report. Clin Case Rep. 202320, 11:8233. 10.1002/ccr3.8233
9. Mbaba AN, Abdalla KM, Ahmed HM: Lentiform fork sign: A distinctive neuroradiologic manifestation of uremic encephalopathy—A case report. Int J Case Rep Images. 2024, 15:81-84. 10.5348/101476Z01AM2024CR
10. Sechi G, Serra A: Wernicke's encephalopathy: new clinical settings and recent advances in diagnosis and management. Lancet Neurol. 2007, 6:442-455. 10.1016/S1474-4422(07)70104-7
11. Kang EG, Jeon SJ, Choi SS, Song CJ, Yu IK: Diffusion MR imaging of hypoglycemic encephalopathy. AJNR Am J Neuroradiol. 2010, 31:559-64. 10.3174/ajnr.A1856
12. Fugate JE, Claassen DO, Cloft HJ, Kallmes DF, Kozak OS, Rabinstein AA: Posterior reversible encephalopathy syndrome: associated clinical and

Volume 8, Issue 6; November-December 2025; Page No 445-459

radiologic findings. Mayo Clin Proc. 2010, 85:427-32. 10.4065/mcp.2009.0590
13. Lambeck J, Hieber M, Dreßing A, Niesen W: Central pontine myelinolysis and osmotic demyelination syndrome. Dtsch Arztebl Int. 2019, 116:600-606. 10.3238/arztebl.2019.0600
14. Ahmed A, Asimi R, Sharma A, Nazir S: Diagnosis: Osmotic myelinolysis (central pontine myelinolysis and extrapontine myelinolysis). Ann Saudi Med. 2007, 27:308-11.
15. Starkey J, Kobayashi N, Numaguchi Y, Moritani T: Cytotoxic Lesions of the Corpus Callosum That Show Restricted Diffusion: Mechanisms, Causes, and Manifestations. Radiographics. 2017, 37:562-576. 10.1148/rg.2017160085
16. Tetsuka S: Reversible lesion in the splenium of the corpus callosum. Brain Behav. 2019, 9:01440.
17. Sharma V, Nayak S, Pattnaik SS, Mohanty AP, Patro S: Snake Bite-Induced Leukoencephalopathy: A Rare Case. Cureus. 2024, 28:55116. 10.7759/cureus.55116
18. Chaudhary SC, Sawlani KK, Malhotra HS, Singh J: Snake bite-induced leucoencephalopathy. BMJ Case Rep. 2013, 18:2012007515.
19. Huang YK, Chen YC, Liu CC, Cheng HC, Tu AT, Chang KC: Cerebral Complications of Snakebite Envenoming: Case Studies. Toxins (Basel. 2022, 27:436. 10.3390/ toxins14070436
20. Reis E, Coolen T, Lolli V: MRI Findings in Acute Hyperammonemic Encephalopathy: Three Cases of Different Etiologies: Teaching Point: To recognize MRI findings in acute hyperammonemic encephalopathy. J Belg Soc Radiol. 2020, 30:9. 10.5334/jbsr.2017
21. Sparacia G, Anastasi A, Speciale C, Agnello F, Banco A: Magnetic resonance imaging in the assessment of brain involvement in alcoholic and nonalcoholic Wernicke's encephalopathy. World J Radiol. 2017, 28:72-78. 10.4329/wjr.v9.i2.72
22. Wakrim S, El Mekkaoui A, Benlenda O, Nainia K, Nassik H: Brain MR imaging in acute hyperammonemic: Case report. Radiol Case Rep. 202220, 17:4046-4048.
23. Butterworth RF: Hepatic encephalopathy. In: Arias IM, Boyer JL, Felsher R, editors. The Liver: Biology and PathobiologyHoboken (NJ): John Wiley & Sons. 2020618638.
24. Warrell DA: Snake bite. Lancet. 2010, 375:77-88. 10.1016/S0140-6736(09)61754-2
25. Kafritsa Y, Fell J, Long S, Bynevelt M, Taylor W, Milla P: Long-term outcome of brain manganese deposition in patients on home parenteral nutrition. Arch Dis Child. 1998, 79:263-5.
26. Rossi NP, Sathyanarayanan G, Mahmood M, Shakespeare D: Toxic leukoencephalopathy versus delayed post-hypoxic leukoencephalopathy after oral morphine sulphate overdose. BMJ Case Rep. 2023, 27:255291.
27. Stamm B, Lineback CM, Tang M, Jia DT, Chrenka E, Sorond F, Sabayan B: Diffusion- Restricted Lesions of the Splenium: Clinical Presentation, Radiographic Patterns, and Patient Outcomes. Neurol Clin Pract. 2023, 13:200196. 10.1212/CPJ.0000000000200196
28. Ahmed SM, Khan M, Zaka-Ur-Rab Z, Nadeem A, Agarwal S: Hypertensive encephalopathy following snake bite in a child: A diagnostic dilemma. Indian J Crit Care Med. 2013, 17:111-2.
29. Basak RC: A case report of Basal Ganglia calcification - a rare finding of hypoparathyroidism. Oman Med J. 2009, 24:220-2. 10.5001/omj.2009.44
30. De Oliveira AM, Paulino MV, Vieira APF, et al.: Imaging patterns of toxic and metabolic brain disorders. Radiographics. 2019, 1:1672-95. 10.1148/rg.2019190016

Volume 8, Issue 6; November-December 2025; Page No 445-459